Automated MRI-Based Biventricular Segmentation Using 3D Narrow-Band Statistical Level-Sets

G Tarroni[1], D Marsili[1], F Veronesi[1], C Corsi[1], AR Patel[2], V Mor-Avi[2], C Lamberti[1]

[1]University of Bologna, Bologna, Italy
[2]University of Chicago, Chicago, Illinois, USA

Abstract

The goal of this study was to develop a near-automated technique for the segmentation of left ventricular (LV) endo- and epicardial as well as right ventricular (RV) endocardial contours from cardiac magnetic resonance (CMR) images. The newly developed technique was tested against conventional manual tracing. Our approach is based on a 3D narrow-band statistical level-set algorithm (applied to a stack of CMR short-axis images) followed by several refinement steps. This technique was tested on steady-state free precession (SSFP) CMR images acquired during 10-15 sec breath-holds in 6 patients, including a total of 120 images. Computational time was around 3 min for a stack of 10 slices. For performance evaluation, an experienced interpreter manually traced ventricular contours on all the images. Quantitative error metrics (Hausdorff distance, HD; mean absolute distance, MAD, Dice coefficient, DC) were computed between automatically identified and manually traced contours. Bland-Altman and linear regression analyses were also performed between automatically and manually computed ventricular volumes. The results (MAD: LV Endo = 1.3±0.7 px, RV Endo = 1.7±1.2 px, LV Epi = 1.5±0.7 px) indicate that fast and accurate identification of LV and RV contours using 3D narrow-band statistical level-sets is feasible.

1. Introduction

Cardiac Magnetic Resonance (CMR) imaging has become the reference technique for the quantification of volumes and masses for both left and right ventricles (LV, RV). The evaluation of LV function is fundamental for the assessment of cardiomyopathies, as well as ischemic and valvular heart diseases, while the estimation of LV mass is important from a prognostic point of view [1]. On the other hand, the assessment of the RV function and morphology is an integral part of the evaluation of patients with pulmonary hypertension, congenital heart disease and ischemic disease affecting the RV itself [2-3].

The quantification of ventricular volumes and masses requires the identification of ventricular contours (i.e. endo- and epicardial contours) on all the acquired slices. The use of conventional manual tracing procedures has proven to be time-consuming and operator-dependent, making these measurements unsuitable for routine clinical use. As a consequence, in the last decade, research efforts have been directed towards the development of automated techniques for the identification of ventricular contours [4]. Despite the availability of commercial software packages dedicated to ventricular segmentation, the problem remains only partially solved, in particular for the right ventricle (because of its unique shape and prominent endocardial trabeculae). This is indicated for example by the RV segmentation challenge at the 2012 MICCAI conference.

Our goal was to develop a near-automated technique for the segmentation of the LV endo- and epicardial contours, as well as the RV endocardial contours. This technique is based on a 3D narrow-band statistical level-set algorithm followed by several refinement steps, which involve anisotropic filtering, 2D edge-based level-set algorithms, and convex hull closing. In this study we tested this novel technique against manual analysis, in terms of accuracy of both contour detection and volume measurement.

2. Methods

2.1. Image analysis

The proposed technique consists of the following macro-steps (figure 1): A) image stacking, B) seeding, C) LV and RV endocardial segmentation, D) LV epicardial segmentation, E) surface reconstruction. Of note, the LV and RV endocardial segmentation processes in step C are performed using the same algorithm.

A. Image Stacking. For each frame, the acquired images are stacked according to their slice location to produce a 3D data matrix, which mimics volumetric acquisition. In order to avoid unnecessary image analysis,

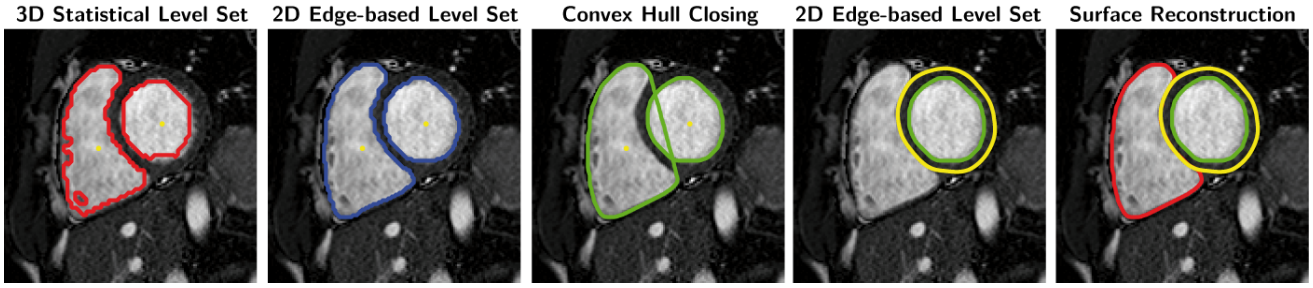

Figure 1. Main steps of the 3D segmentation technique shown in one slice.

the user selects the range of slices, which display the ventricular cavities.

B. Seeding. The user is asked to manually place two seed points, one inside each ventricular cavity, in a random slice.

C. LV and RV endocardial segmentation. The first step of endocardial segmentation consists of the application of a 3D narrow-band statistical level-set algorithm. The level-set function φ: $\Omega \subset \mathbb{R}^3 \rightarrow \mathbb{R}$, initially corresponding to a 2-px-radius sphere centered in the previously positioned seed point, evolves in time in order to minimize a defined energy functional. In the narrow-band implementation, the evolution of each small portion of the interface represented by φ depends only on locally computed statistics [5]. From a mathematical point of view, the energy functional to be minimized is defined by:

$$E(\varphi) = \int_{\Omega} \delta(\varphi(x)) \int_{\Omega} W(x,y) F\left(I(y), \varphi(y)\right) dxdy + \mu \int_{\Omega} \delta(\varphi(x)) \left\| \nabla \varphi(x) \right\| dx$$

where δ is the Dirac function, I is the slice stack obtained in step A, x and y are the spatial coordinates of points inside the stack, F indicates the type of statistics to be computed, μ weights a regularization term and W, which is defined as:

$$W(x,y) = \begin{cases} 1, & if\ |x-y| < \rho \\ 0, & otherwise \end{cases},$$

is a mask function (of radius ρ) which achieves the narrow-band evolution. The adopted functional F follows the Maximum Likelihood criterion [6]. This statistical approach relies on the a priori knowledge of the type of noise distribution of the dataset in order to segment the different components. The functional is defined as:

$$F(I,\varphi) = -\left(\int_{\Omega_i} \log p(I)\, dx + \int_{\Omega_o} \log p(I)\, dx \right)$$

in which Ω_i and Ω_o are respectively the inner and outer domain relatively to the interface and p(I) is the probability density function of the gray levels in the dataset, which is approximately Gaussian for CMR images. The algorithm is completed with appropriate boundary conditions and runs until convergence. The second step consists of contour refinement by means of anisotropic filtering, followed by a 2D edge-based level-set algorithm. Each slice I_s contained in I undergoes an anisotropic filtering, which aims at denoising the image without altering the edges. The filtering procedure is based on the following equation:

$$\frac{dI_s}{dt} = gK \left\| \nabla I_s \right\| + \nabla g \cdot \nabla I_s$$

where K is the curvature (computed on the isocurves of I_s) and g is the Perona-Malik edge indicator function [7]. Then, for each slice, a 2D edge-based level-set algorithm is applied to the previously computed contours (ridefined as φ_s) following the Malladi-Sethian formalism:

$$\frac{\partial \varphi_s}{\partial t} = g(\varepsilon K - o) \left\| \nabla \varphi_s \right\| + \nu \nabla g \cdot \nabla \varphi_s$$

where g is the edge indicator applied to the filtered slices and ε, o and ν are weighting factors for the curvature, the balloon and the advection evolution terms, respectively [8]. Once the algorithm has reached convergence, to further refine the contours and to help including in the endocardial boundaries, papillary muscles and endocardial trabeculae, the previously computed contours undergo a convex hull closing in each slice.

D. LV epicardial segmentation. Starting from the computed LV endocardial contours, a 2D edge-based level-set algorithm is applied, following the above Malladi-Sethian formalism. At convergence, each contour undergoes a final regularization step performed using a curvature-based motion. [9].

E. Surface reconstruction. In order to restore the normal concavity of the RV, which might have been altered by the convex hull closing, in each slice, the overlapping area between the LV epicardial contour and the RV endocardial contour is subtracted from the latter.

2.2. Image acquisition

A 1.5 T scanner (Achieva, Philips™), equipped with a phased-array cardiac coil, was used to acquire cine-loops in short-axis view during 10 to 15 sec breath-holds using the steady-state free precession (SSFP) dynamic

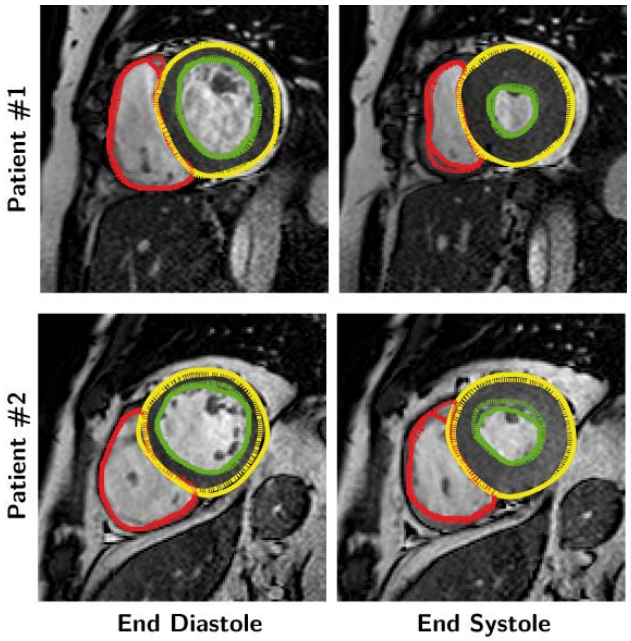

Figure 2. Example of visual comparison between the automatically and the manually identified contours in two slices acquired in two different patients at end-diastole and end-systole. The automatically identified contours are represented with solid lines, while manually drawn contours are depicted with dashed lines.

gradient-echo mode sequence. The number of slices ranged from 13 to 20, from the base to the apex (8 mm slice thickness, no gaps) and the temporal resolution was 30 frames per cardiac cycle. In-plane resolution ranged from 1.172 to 1.484 mm.

2.3. Performance testing

The technique was tested on both end-diastolic (ED) and end-systolic (ES) frames from 6 different subjects (3 males; age 34 ± 15 yrs), with the total number of analyzed images equal to 120. To test the performance of the proposed technique, an experienced interpreter, blinded to the results of the automated analysis, manually traced LV and RV endo- and LV epicardial contours in all images. To assess the accuracy of the technique, several error metrics were computed between the automatically identified and manually traced contours. These metrics were: the Hausdorff distance (HD), the mean absolute distance (MAD) and the Dice coefficient (DC) [10]. The first two indices estimate respectively the maximum and the mean distance in pixels between the two contours, while the Dice coefficient represents the normalized size of the overlapping area between them. These metrics were computed between the automatically and manually identified LV endocardial contours, the RV endocardial contours and the LV epicardial contours, respectively, and finally averaged among all the analyzed images. Finally, Bland-Altman and linear regression analyses with Pearson's correlation coefficient were performed to compare ventricular volumes computed from automatically and manually identified contours.

3. Results

Time required for the near-automated identification of the LV endo- and epicardial contours as well as the RV endocardial contours in a stack of 10 slices was around 3 minutes on a 2.8 Ghz Quad-Core Intel Xeon® PC with 8 GB of RAM. Of note, the LV and RV 3D narrow-band level-set algorithms, which are the most time-consuming part of the automated technique, were run in sequence, although they could easily be executed in parallel, thus reducing the computation time. In comparison, the manual segmentation of the same stack of 10 slices required around 15 minutes. Figure 2 shows an example of the comparison between automatically identified and manually traced contours. Table 1 shows the summary of results for the computed error metrics for the different contours. Of note, in 15 slices (always towards the apical level) the comparison was not performed due to the inability of the automated technique to identify endocardial contours. Table 2 presents the results of Bland-Altman analysis in terms of biases, standard deviations and mean measured values in ml. The results for Pearson's correlation coefficients and linear regression analysis are reported in figure 3.

	HD (px)	MAD (px)	DC (a.u.)
LV Endocardial Contours	3.4 ± 1.7	1.3 ± 0.7	0.9 ± 0.1
RV Endocardial Contours	6.6 ± 4.6	1.7 ± 1.2	0.8 ± 0.2
LV Epicardial Contours	3.6 ± 1.5	1.5 ± 0.7	0.9 ± 0.0

Table 1. Results of the comparisons between automatically and manually identified contours for the selected error metrics (mean±SD).

	Bias	Std	Mean Value
LV Endocardial Volume	-8.46	5.77	110.08
RV Endocardial Volume	-9.04	8.41	100.19
LV Epicardial Volume	20.16	18.01	255.22

Table 2. Results of the Bland-Altman analysis between automatically and manually computed volumes. All the values are reported in ml.

4. Discussion and conclusions

This study aimed at developing a technique for the near-automated segmentation of LV endo- and epicardial contours as well as RV endocardial contours in

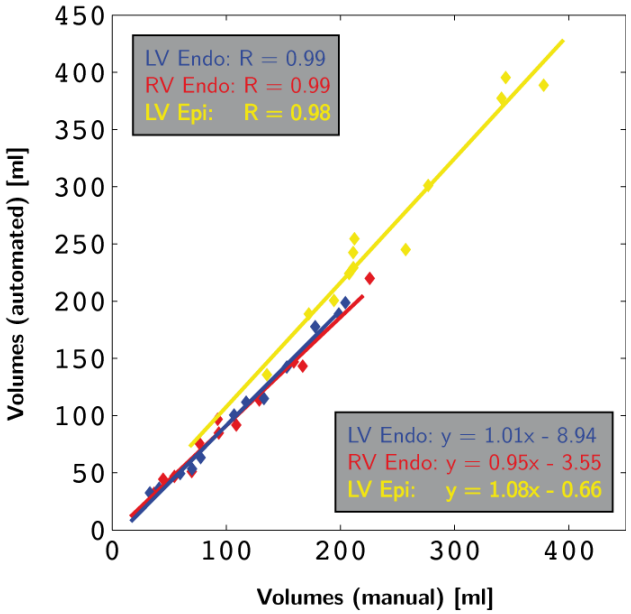

Figure 3. Pearson's correlation coefficients and results of the linear regression analysis between automatically and manually computed volumes.

CMR images, and testing its accuracy against conventional manual tracing. Despite many research efforts and the presence of commercially available software programs, the automated identification of the ventricular contours as a basis for the quantification of cardiac volumes and masses can still be considered an unsolved issue. This is especially true for the RV segmentation, hindered by its more irregular shape, its usually high density of trabeculae and the frequent presence of pericardial fat (which has image intensity similar to that of the ventricular cavity). The technique proposed in this study is based on a 3D narrow-band statistical level-set algorithm, followed by a series of refinement steps. The identification of both LV and RV endocardial contour is performed using the same technique, and the only manual input required is the positioning of a seed point inside each ventricular cavity in one random slice.

The results obtained in this pilot study demonstrated in a small number of subjects the high accuracy of the proposed technique. This was particularly indicated by the mean absolute distance, which was around 1.5 px on average for all the three types of contours. Moreover, Bland-Altman and linear regression analyses showed excellent inter-technique agreement (R from 0.98 to 1.00) and relatively small biases.

The main limitation of this study is the small number of subjects whose images were used to test our approach. To address this issue, we are planning on validating this approach in larger groups of patients with normal as well as abnormal LV and RV sizes and function.

In conclusion, fast and accurate identification of LV and RV contours using the described approach is feasible, and could potentially lead to the implementation of a reliable near-automated tool for the quantification of LV and RV volumes and LV mass from CMR images.

References

[1] Schillaci G, Verdecchia P, Porcellati C, Cuccurullo O, Cosco C, Perticone F. Continuous relation between left ventricular mass and cardiovascular risk in essential hypertension. Hypertension 2000; 35(2): 580–586.

[2] Davlouros PA, Niwa K, Webb G, Gatzoulis MA. The right ventricle in congenital heart disease. Heart 2006; 92(Suppl 1): i27–38.

[3] Chin KM, Kim NHS, Rubin LJ. The right ventricle in pulmonary hypertension. Coronary artery disease 2005; 16(1):13–8.

[4] Petitjean C, Dacher J-N. A review of segmentation methods in short axis cardiac MR images. Medical image analysis 2011; 15(2):169–84.

[5] Lankton S, Tannenbaum A. Localizing region-based active contours. IEEE Trans Im Proc 2008; 17(11):2029–39.

[6] Sarti A, Corsi C, Mazzini E, Lamberti C. Maximum likelihood segmentation of ultrasound images with Rayleigh distribution. IEEE Trans Ultrason Ferroelectr and Freq Contr 2005; 52(6):947–60.

[7] Perona P, Malik J. Scale-space and edge detection using anisotropic diffusion. IEEE Trans PAMI 1990; 12(7).

[8] Sethian JA. Level set methods and fast marching methods. Cambridge: Cambridge University Press; 1999.

[9] Caiani EG, Redaelli A, Parodi O, Votta E, Maffessanti F, Tripoliti E, Nucifora G, De Marchi D, Tarroni G, Lombardi M, Corsi C. Development and validation of automated endocardial and epicardial contour detection for MRI volumetric and wall motion analysis. Comput Cardiol 2010; 37: 1083-1086.

[10] Ghosh P, Sargin ME, Manjunath BS. Robust dynamical model for simultaneous registration and segmentation in a variational framework: A Bayesian approach. 2009 IEEE 12th Conference on Computer Vision, 709–716.

Address for correspondence:

Giacomo Tarroni, PhD
University of Bologna
Viale Risorgimento 2, 40136 Bologna, Italy
giacomo.tarroni@unibo.it